Analytic representation of the proton-proton and proton-nucleus cross-sections and its application to the sea-level spectrum and charge ratio of muons

G. D. Badhwar, S. A. Stephens,* and R. L. Golden
National Aeronautics and Space Administration, Johnson Space Center, Houston, Texas 77058
(Reveived 5 January 1976; revised manuscript received 8 October 1976)

We have calculated the sea-level differential muon momentum spectrum and their charge ratio from 1 GeV/c to 5000 GeV/c, using all of the available accelerator data. We find an excellent agreement between our calculation and the existing experimental data. We see no need, at present, to invoke any change either in the cosmic-ray chemical composition or in the nature of the hadron-nucleus interaction at hadron energies above 1500 GeV.

I. INTRODUCTION

The cosmic-ray sea-level muon momentum spectrum and charge ratio, μ^+/μ^-, can be calculated from a detailed knowledge of the characteristics of hadron-nucleus collisions and the composition of the primary cosmic-ray nuclei at the top of the atmosphere. A comparison of the calculated and observed muon spectrum and charge ratio can then be used as a tool to explore the nature of the hadronic interaction or the cosmic-ray composition as a function of momentum. A number of calculations[1-8] have been done, some very recently, to calculate the charge ratio, with divergent results. However, only now do we have extensive and reliable data on the basic hadron-hadron interactions, so that the production spectra of pions and kaons can be calculated accurately. It is in the description of nuclear effects, that is, in hadron-nucleus collisions, that one is forced to use models, and we believe this to be the main source of inaccuracy in previous calculations. Moreover, calculations of the *absolute* sea-level differential muon spectrum have not been done in the past. It is thus felt that a self-consistency check between the absolute spectrum and charge ratio of muons has not been made in any of the earlier calculations.

In this paper we have calculated the differential muon momentum spectrum and the muon charge ratio from about 1 to 5000 GeV/c, from first principles, using all of the available accelerator data. We have developed, by making use of the experimental data, a representation of $\pi^{\pm}$, $K^{\pm}$ invariant cross sections for proton-proton collisions for incident proton energies from 6.6 to about 1500 GeV. This representation has been extended to hadron-nucleus interaction by introducing a new parameter, which we have determined from the existing data on beryllium, aluminum, and lead targets. We have thus avoided using any model to account for nuclear effects. Making use of these representations and the observed cosmic-ray chemical composition, and taking into account the variation of scale height with atmospheric depth (in contrast to an isothermal atmosphere in previous calculations), we have calculated the absolute muon intensity and the muon charge ratio as a function of the muon momentum.

II. REPRESENTATION OF THE $\pi^{\pm}$, $K^{\pm}$ INVARIANT CROSS SECTION

The quantity of direct interest in our calculation is the differential cross section, $(d\sigma/dE)(E, E_0)$, for the production of pion or kaon of energy E from a proton of energy E_0. This is related to the invariant cross section, $(Ed^3\sigma/d^3p)$, by the relation $d\sigma/dE \simeq (\pi/p_{\parallel})\int E(d^3\sigma/d^3p)dp_{\perp}^2$, where $p_{\parallel}$ is the parallel component of the laboratory momentum.

In Fig. 1(a), we have plotted the experimental data,[9-13] on the π^+ invariant cross section, $Ed^3\sigma/d^3p$, at fixed value of $p_{\perp}$ as a function of the variable

$$\tilde{x} \simeq \left[x_{\parallel}^{*2} + \frac{4}{s}(p_{\perp}^2 + m_{\pi}^2) \right]^{1/2}$$

for incident proton energies of 6.6, 12, 24, 200, 1100, and 1500 GeV. Here $x_{\parallel}^*$ is the ratio of the parallel component of the center-of-mass (c.m.) momentum to the maximum transferable momentum and $\sqrt{s}$ is the total energy in the c.m. system. Figure 1(b) similarly shows the π^- invariant cross section at proton energies of 12, 24, 300, 1100, and 1500 GeV, respectively. The solid circles are for $p_{\perp} = 0.2$ GeV/c, the solid triangles are for $p_{\perp} = 0.4$ GeV/c, and the solid squares are for $p_{\perp} = 0.8$ GeV/c. It is clear that for a fixed $p_{\perp}$, the invariant cross section is a power law in $(1-\tilde{x})$. Inspired by the Regge-Mueller behavior of the invariant cross section and the success of Carey *et al.*[11] in fitting part of the π^0 cross section, we have fitted the $\pi^{\pm}$ data to the expression

$$(Ed^3\sigma/d^3p) = A/(1+4m_p^2/s)^r \times (1-\tilde{x})^q \exp[-Bp_{\perp}/(1+4m_p^2/s)], \quad (1)$$

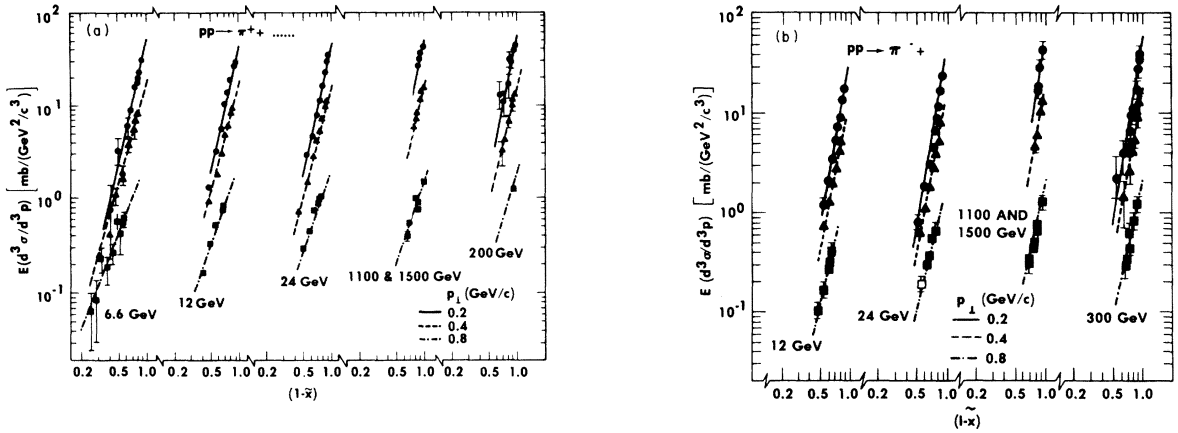

FIG. 1. (a) A plot of the π^+ invariant cross section, $Ed^3\sigma/d^3p$, as a function of $1-\tilde{x}$. The solid circles are for $p_\perp = 0.2$ GeV/c, the solid triangles are for $p_\perp = 0.8$ GeV/c, and the solid squares are for $p_\perp = 0.8$ GeV/c. The lines through the data points are calculated using Eq. (1). (b) A plot of the π^- invariant cross section as a function of $1-\tilde{x}$ at fixed values of $p_\perp$. The symbols are the same as in (a).

where q is a function of $p_\perp$ and s such that

$$q = (C_1 + C_2 p_\perp + C_3 p_\perp^2)/(1 + 4m_p^2/s)^{1/2}. \quad (2)$$

The constants A, B, C_1, C_2, and C_3 and r are given in Table I. It can be seen that this equation has the right threshold behavior. From these data, it is not possible to establish the $p_\perp$ dependence above $p_\perp$ of 0.8 GeV/c. However, this should have negligible effect on our calculation of $d\sigma/dE$, because the cross section is very small at $p_\perp > 0.8$ GeV/c. We note from Table I that the $(1-\tilde{x})$ dependence of the cross section for π^- is steeper than for π^+. In Fig. 2, we present the data[12,14] on the total production cross section for π^+ (filled points) and π^- (open points). The solid curves marked A and B are calculated using Eq. (1), and this figure clearly shows the good agreement between the calculated cross section and the observed data. Thus the representation of Eq. (1) not only gives the differential invariant cross section, it also gives the correct total cross section. We thus believe that we can reliably calculate $d\sigma/dE$ for any E and E_p.

We have shown in Fig. 3 a plot of the data taken from Yen[15] on kaon invariant cross sections for various values of $p_\perp$ and at different incident proton energies ranging from 12.2 to 1500 GeV. The solid curves shown in this figure are the calculated cross sections using the representation $Ed^3\sigma/d^3p = A(1-\tilde{x})^C \exp(-Bp_\perp)$, where A, B, and C are constants and are given in Table I for both K^+ and K^-. One can notice that the above representation gives a good fit to the observed data.

In order to extend our representations to collisions of protons with air nuclei, we have made use of the existing data[16-20] on collisions of protons on beryllium, aluminum, and lead targets for incident proton energy between 12 and 300 GeV. In Fig. 4, we have shown the ratio of invariant cross sections $R = (Ed^3\sigma/d^3p)_{\pi^+}/(Ed^3\sigma/d^3p)_{\pi^-}$ as a function of the fractional pion energy E_π/E_p ($\propto x_\parallel^*$) for 18.8-, 23.1-, and 200-GeV incident proton energy; the filled data points refer to the hydrogen target, while the open symbols correspond to the beryllium target. It is evident from this figure that the ratio R for the beryllium target is systematically smaller than that for the hydrogen target. In particular, this difference increases for large (E_π/E_p) values indicating this effect is not resulting from nuclear cascading within the nucleus, which

TABLE I. Parameters for the representation of invariant cross section.

Particle	A [mb/(GeV^2/c^3)]	B	r	C [(GeV/c)$^{-1}$]	C_1	C_2 [(GeV/c)$^{-1}$]	C_3 [(GeV/c)$^{-2}$]
π^+	153	5.55	1	...	5.3667	−3.5	0.8334
π^-	127	5.3	3	...	7.0334	−4.5	1.667
K^+	8.85	4.05	...	2.5	...	...	...
K^-	9.3	3.8	...	8.3	...	...	...

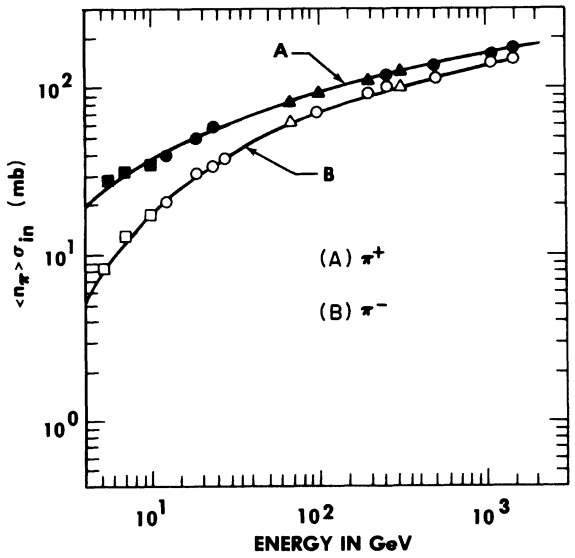

FIG. 2. A plot of π^+ and π^- total production cross section as a function of the incident proton energy. Curves A and B are calculated using Eq. (1) for π^+ and π^-, respectively. The data points triangles are taken from Whitmore (Ref. 12), and squares and circles are from Bracci *et al.* and Antinucci *et al.*, respectively, in Ref. 14.

would lead to the production of low-energy pions. The observed decrease can be understood if for a certain fraction, η, of p-n collisions, inside the nucleus, the incoming proton undergoes charge exchange with the target neutron and behaves like a neutron; the resulting ratio, R_{pn}, in the forward direction is the same as the ratio, R_{nn}, for nn collisions. We have envisioned this phenomenon to take place "essentially" before pion production occurs on the same target neutron. In the remaining fraction $(1-\eta)$ of pn collisions the ratio R in the forward direction is the same as that of pp collisions. We define η as the *charge-mixing parameter*; this mixing of charge between the incoming and target nucleons does not alter the characteristics of pp or nn collisions. A complimentary situation exists for np collisions. We wish to emphasize that η is not a rescattering correction in the Glauber model, but a phenomenological parameter.

Thus, for p-nucleus collisions, it follows that the invariant cross section per target nucleon for the production of π^+ and π^- can be effectively represented as

$$(Ed^3\sigma/d^3p)_{\pi^\pm} = \lambda_{pp}[p_+ + \eta f_n(p_\pm - p_\pm)]/\lambda_{pN},$$

where p_+ and p_- are the invariant cross sections, respectively, of π^+ and π^- in pp collisions and f_n is the fraction of neutrons in the target nucleus (here we have used the fact that $R_{pp} = R_{nn}^{-1}$), and λ_{pp} and λ_{pN} are the interaction mean free paths for pp and p-nucleus collisions. From the above relation, one can evaluate the charge-mixing parameter

$$\eta = (R_{pp} - R_{pN})/[(R_{pp} - 1)(R_{pN} + 1)f_n],$$

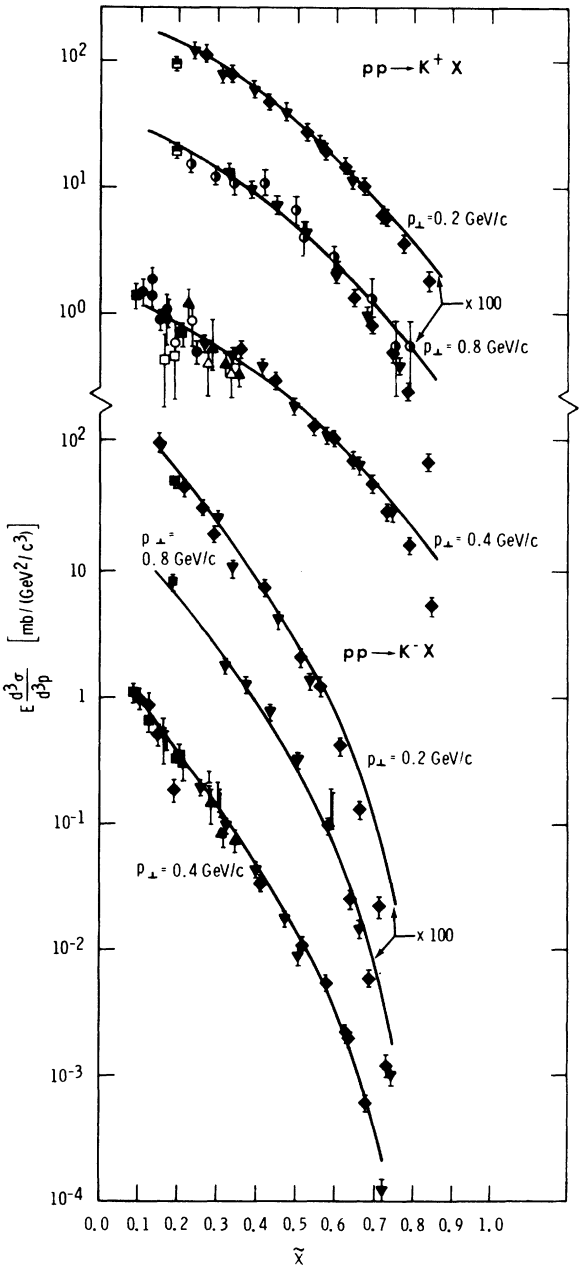

FIG. 3. A plot of the invariant cross section, $Ed^3\sigma/d^3p$, for both K^+ and K^- versus $\tilde{x} = E^*/E^*_{max}$. The data are taken from Yen (Ref. 15) and the solid lines correspond to our calculations using Eq. (2).

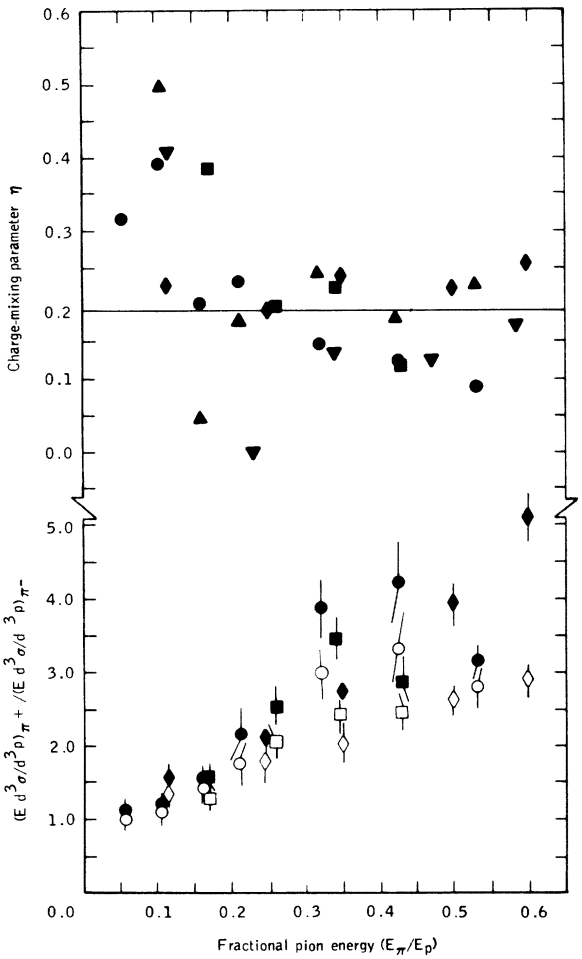

FIG. 4. The lower part of this figure shows the ratios of invariant cross sections for the production of π^+ and π^- with hydrogen target (filled data points) and on beryllium targets (open data points) as a function of the fractional pion energy ($\simeq\tilde{x}_{\parallel}$) by incident protons of energies 18.8, 23.1, and 200 GeV. The upper part of this figure shows the calculated values of the charge-mixing parameter η as a function of the fractional pion energy for p-Be interactions at various incident proton energies; the solid line corresponds to the weighted mean value of η. The symbols are as follows: ● 18.8 GeV, 0.0 mrad; ▲ 18.8 GeV, 100 mrad; ■ 23.1 GeV, 0.0 mrad; ◆ 200 GeV, 3.6 mrad; and ▼ 300 GeV, 3.6 mrad.

where R_{pN} is the π^+ and π^- ratio in p-nucleus collisions. In Fig. 4, we have plotted the values of η, evaluated for the beryllium target, as a function of E_π/E_p for different incident energies. The errors in the points vary from about 20% to more than 100% and are not indicated in the figure. The weighted mean value of η is found to be 0.195 ± 0.015 and is shown by the solid line; the points which are far away from the mean value have large errors. A similar determination of η using the data for the lead target[17] gives $\eta = 0.18 \pm 0.05$ at 23.1 GeV, which can be compared to 0.19 ± 0.03 for the beryllium target at the same proton energy.[21]

As noted earlier, the data used in determining η are for proton energies greater than 18.8 GeV and show η to be independent of energy above this energy. There are some new data of Edge *et al.*[22] at energies of 1.94, 2.94, and 3.94 GeV on Be, C, and Pb targets. A comparison of the π^+/π^- ratio from these data at 3.94 GeV with that from Melissinos *et al.*[23] for pp collisions at 2.84 GeV gave a value for η about 0.45, considerably higher than the value above 18.8 GeV. From a similar comparison at 1.94 GeV with the ratio of total cross sections of π^+ to π^- productions for pp collisions, we obtained a value of 0.4 for η. Thus, there is an indication that η increases at low energies. Within the uncertainties of the derived values, we have assumed that η has an energy dependence of the type $\eta(s) = \eta_0(1 + 8.5/s)$, where η_0 is the value derived above 18.8 GeV.

Thus by using a single parameter, η, which has been determined from experimental data, our pp-collision representation can be extended to p-nucleus collisions.[24] It might be noted that such a model violates the hypothesis of limiting fragmentation in which the ratio of π^+/π^- is determined by the incident particle alone. However, it has been already shown that the hypothesis of limiting fragmentation is not valid in detail either in describing the invariant cross section or the charge transfer (exchange) probability.[9] In our calculations, we assumed that the K^+/K^- ratio is also affected in a similar manner. Further, all these representations are considered to hold good at energies higher than the CERN ISR energy of ~1500 GeV, the validity of which would only affect the muon calculations above a muon energy of ~150 GeV. We do not make any explicit assumptions regarding scaling or limiting-fragmentation hypotheses; however, the assumed validity of the above representation at proton energies above 1500 GeV implies scaling in terms of the set of variable $(E^*/E^*_{\max}, p_\perp)$ and *not* in the conventional Feynman-Yang scaling variables $(p^*/p^*_{\max}, p_\perp)$.

We have used the experimentally verified fact that π + nucleon → π + anything is similar to p + nucleon → π + anything in evaluating the effects of pion-induced reactions. In particular, we note that at 205 GeV/c the average charge particle multiplicity in πp is 8.00 ± 0.17 compared to 7.65 ± 0.17 for pp collisions.[9,25] These representations have been used in the calculation of the production spectrum of pions and kaons.

III. PRODUCTION SPECTRUM OF PION AND KAONS

The production spectrum of pions or kaons per g cm^{-2} as a function of atmospheric depth, X, is given by

$$P_j(E,X)=\sum_i \frac{f_i}{\lambda_i}\int_E^\infty \frac{d\sigma_j}{dE}(E,E_0)J_i(E_0,X)dE_0, \quad (3)$$

where $d\sigma_j/dE$ is the differential production cross section of the j-type particle (pion or kaon) described in Sec. II above, f_i is the fraction of interacting nucleons, and $J_i(E_0,X)$ is the differential flux at X of the cosmic nuclei of ith type with an interaction mean free path, λ_i, in air. From a summary of the existing data on the differential energy spectrum of the proton[26,27], we have found

$$\begin{aligned} J_p(E_0) &= 8.6\times10^3 E_0^{-2.55}, \quad 1.2\le E_0\le 68 \text{ GeV} \\ &= 2.0\times10^4 E_0^{-2.75}, \quad E_0\ge 68 \text{ GeV}, \end{aligned} \quad (4)$$

where E_0 is the total proton energy and $J(E_0)$ is in protons/(m^2 sr sec GeV), and provides a best fit to the data. For helium nuclei, all of the available data can be described as a power law in rigidity of the form $J_\alpha(R)=CR^{-2.75}$, where C is determined by the requirement that at 50 GeV/nucleon $J_\alpha(E)/J_p(E)=4.3\%$.[26] It should be noted that there could be a systematic error of about 20% in the flux (above 68 GeV) given by Eq. (4), though the relative abundance of protons to helium is not in error.[26] The chemical composition of Juliusson[28] for $Z\ge 3$ was used. The deuteron flux is not very well known. However, based on the fragmentation of ^{4}He we expect to have a ^{2}H/H $\approx 1.5\%$ at the same kinetic energy per nucleon[29]; this value has been assumed in our calculations. Thus we find that the fraction of neutrons in cosmic radiation above 68 GeV is 0.105.

The fraction of participating nucleons f_α in an interaction of helium nuclei is available experimentally[30] and, for convenience, all the heavy nuclei have been replaced by an equivalent number of helium nuclei (see Appendix). In this respect we also take account of the change of composition as a function of atmospheric depth due to fragmentation. Further, since the spectra of protons and heavy nuclei are not simple power laws in kinetic energy per nucleon, the spectral shapes slowly change with depth as a result of finite inelasticity. This enhances the production of low-energy pions and kaons at large depths.

The charge ratios of pions and kaons at production were estimated as a function of atmospheric depth by first determining the charge excess $\delta(X)$ in the interacting nucleons, which is defined as the fraction $(p-n)/(p+n)$, by the relation[31] $\delta(X)=\delta(0)\exp[2wX(1/\Lambda-1/\lambda)]$, where $\delta(0)$ is the charge excess in a given component of primary cosmic-ray nuclei and w is the charge-transfer probability. Here we have taken into account the observed increase of the inelastic p-p cross section with energy as $\propto 1.125 \ln E$ and the change in the values of Λ resulting from the spectral change in the cosmic-ray nucleons at low energies. However, we have not considered in our calculations the possible increase of the inelastic cross section for pions and kaons since its form is not known very well, and will only marginally affect the muon flux at sea level. The charge-transfer probability w depends on x_{11}^* and the effective value of w, used in the above expression, can be determined if one knows the invariant cross section for the production of proton and neutrons.[3] However, not enough data are available over a wide enough range of incident energies to estimate accurately the effective value of w and its possible dependence on the primary energy. From the study of high-energy jets in emulsion, in the TeV region, Daniel *et al.*[32] found that the value of w is 0.26 ± 0.07, which is consistent with the value of 0.21 calculated by Adair[3] from the invariant cross section at 200 GeV. From the rather poor 300-GeV data of Dao *et al.*,[33] we found that the value of w lies between 0.1 and 0.5. Since the error involved in such estimates is large, we have assumed a value of 0.26 in our calculations. It is also important to note that the effective value of w is expected to approach the total charge transfer probability of 0.5 near threshold energies. Therefore, we have used an energy dependence of the type $w(E)=0.26(1.0+1.8/\sqrt{s})$ for w and discuss its effect later (Sec. V).

The interaction mean free path for protons λ_p in air[34] is taken to be 90 g cm^{-2} and Λ_p, the attenuation mean free path[31] as 125 g cm^{-2} at around 28 GeV. The values of interaction mean free paths of α particles, pions, and kaons[35,36] are taken to be 45, 120, and 150 g cm^{-2}, respectively. Using the production spectra of pions and kaons and their charge ratios as a function of atmospheric depth, their equilibrium spectra in the atmosphere are determined as shown in the Appendix and the sea-level muon spectrum is then calculated as described in Sec. IV. In all of these calculations, the U.S. standard atmosphere has been made use of to take into account the variation of the atmospheric scale height with depth.

IV. DERIVATION

The flux of pions, $F_\pi(E,X)dE$ at any depth, X, is given by the solution of the transport equation[37]:

$$\frac{d}{dX}[F_\pi(E,X)]dE = P_\pi(E,X)dE - \frac{1}{\lambda_\pi}F_\pi(E,X)dE - F_\pi(E,X)dE(U_\pi/EX) + F_\pi(E/q,X)\frac{dE}{q}\frac{1}{\lambda_\pi} + \int_{E'}F_\pi(E',X)dE'\frac{1}{\lambda_\pi}\sigma_\pi(E',E)dE. \quad (5)$$

In this equation the first term on the right-hand side is the production spectrum of pions at depth X. The second term is the loss of pions due to interaction, where λ_π is the interaction mean free path for pions. The third term is the loss of pions due to decay, where $U_\pi(X) = h_0(X)m_\pi/cT_\pi$; $h_0(X)$ is the scale height of the atmosphere and T_π is the lifetime of pions. The fourth term gives the number of pions of energy E/q, which as a result of finite inelasticity during interactions, enters the energy interval dE, where $q = [0.5(E - m_\pi) + m_\pi]/E$ is the elasticity. The last term is the production spectrum of secondary pions as a result of the interaction of pions themselves, where $\sigma_\pi(E',E)$ is the differential cross section for the production of secondary pions of energy E due to the interaction of the primary pion of energy E' in one g cm^{-2} of the atmosphere.

If the slope of the pion spectrum can be approximated by a power law over a range of a factor of 2 in total energy in any given energy domain and if this slope remains the same over a range of depth in which $(X'/X)U_\pi/E$ is approximately a constant, then the solution of the transport equation without the last term can be written as

$$F_\pi(E,X) = \exp\left\{\int_0^X dX'\left[\frac{1-q^{\beta-1}}{\lambda_\pi} + \frac{U_\pi(X')}{X'E}\right]\right\} \times \int_0^X dX'' P_\pi(E,X'') \times \exp\left\{\int_0^{X''} dy\left[\frac{1-q^{\beta-1}}{\lambda_\pi} + \frac{U_\pi(y)}{yE}\right]\right\}. \quad (6)$$

Since $\beta'(E,X)$, the spectral index of the equilibrium pion, is not known explicitly, an iterative procedure has been used. We first determine the pion spectrum by neglecting the fourth term in Eq. (5) and obtain β'. This value of β' is used in Eq. (6) to evaluate the new pion spectrum and the new β'. The last term in Eq. (5) is separately calculated and added to $P_\pi(E,X)$ to finally evaluate the pion spectrum (see Appendix).

From the pion spectrum we obtain the muon production spectrum

$$P_\mu(E,X)dX = \int_{E'}F_\pi(E',X)\frac{U_\pi(X)}{E'}\frac{dX}{X}\frac{dE'}{\psi_\mu(E')},$$

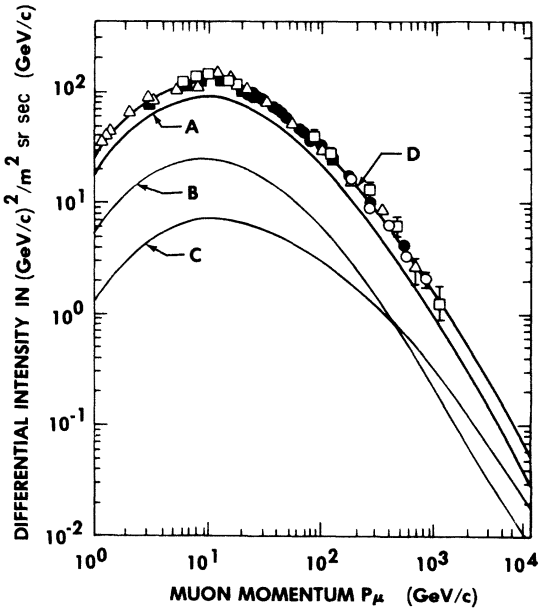

FIG. 5. The differential momentum spectra of sea-level muons are shown in units of (GeV/c)^2/(m^2 sr sec GeV/c). Curves A and B in this figure are the muon spectra resulting from the decay of pions and are from the interactions of cosmic-ray singly charged and heavy nuclei ($Z \geq 2$), respectively. Curve C is from the decay of kaons and the total muon spectrum is represented by curve D. The data points shown in this figure are taken from the following: △ Allkofar *et al.* (Ref. 38), ● Ayre *et al.* (Ref. 39), ○ Baxendale *et al.* (Ref. 40), □ Nandi and Sinha (Ref. 41), and −Abdel-Monem *et al.* (Ref. 42).

where $\psi_\mu(E)$ is taken to be a square distribution function between the minimum and the maximum energies the muon gets from the pion, on the basis of two-body decay kinematics. The limits of the integration are also determined in the same manner. The flux of muons $F_\mu(E,x)dE$ is given by

$$F_\mu(E,X)dE = \int_0^X P_\mu(E',X')[(dE'/dX)/(dE/dX)]dE \times \exp\left\{-\int_{X'}^X \frac{dy}{[yE'(y)/U_\mu(y)]}\right\}dX'. \quad (7)$$

Here the exponential term is the survival probability of a muon from its point of production with energy E', to the point of observation, where its energy is reduced to E by energy-loss processes. In a similar manner, one can express the muon spectrum resulting from kaon decay.

V. RESULTS

In Fig. 5, we show the calculated muon spectrum at sea level from 1 to 6000 GeV/c along with most of the recent data.[38-42] Curves A and B in

this figure are the muon spectra due to the decay of pions from the interactions of cosmic-ray protons and heavier nuclei, respectively, curve C is that due to the decay of kaons, and the total muon spectrum is shown by curve D. One notices the excellent agreement between the calculated and observed muon spectra over the three decades of energy. The contribution of kaon decay to the total muon flux at sea level increases from a few percent around 1 GeV/c to an asymptotic value of about 30% above 10^4 GeV/c. In our calculation, we have taken into account the contribution from neutral kaons, which is $\lesssim 2\%$ of that from pion decay. We have found that the effect of taking the variation of atmospheric scale height is to suppress the flux of low-energy muons at sea level by about 1.5% at 1 GeV/c relative to the high-energy flux, although its effect is much greater on the pion and kaon fluxes.

One observes from Fig. 5 that the shape of the muon spectrum varies slowly over the entire energy range. The differential spectral index of muons from the decay of pions changes from about 0.65 to 1 GeV/c (curve A) to 3.58 at 1000 GeV/c, reaching an asymptotic value of 3.75 only above 10^4 GeV/c. In the case of curve B, the initial spectral index is slightly steeper (0.75) because the incident spectrum is different from that of protons below 68 GeV. On the other hand, muons from the decay of kaons (curve C) have a flatter spectrum (because the probability of decay per gram of the atmosphere for muons is larger than that for pions), with spectral index of about 0.5, which slowly increases to a value of 3.25 at 1000 GeV/c and reaches the asymptotic value well above 10^4 GeV/c. For the combined spectrum, curve D, the spectral index varies from about 0.6 at 1 GeV/c to 3.54 at 1000 GeV/c, which can be compared with the observed values of 0.5 and 3.54, respectively.[38]

The errors in the production cross section for pions and kaons and the error in the effective interaction mean free path for all cosmic-ray nuclei propagate directly into the estimate of the muon flux. However, the effect of the error in the attenuation mean free path is small.[8] The error in our calculated muon spectrum, without taking into account the uncertainty in the primary cosmic-ray spectrum, is estimated to be $<10\%$. Ryan *et al.*[26] have indicated that their measurement of the absolute intensity of cosmic-ray protons and helium nuclei above 50 GeV per nucleon could have a systematic error of about 20%. However, this uncertainty will have no effect on the shape of our calculated muon spectrum or on the charge ratio. In view of the fact that the calculated spectrum is in excellent agreement with observations over the entire energy region, it is plausible that the systematic error in the cosmic-ray spectrum could well be less than 20%; this is what we would expect since the spectra of Ryan *et al.* join smoothly with the low-energy data from measurements made with different techniques.

In Fig. 6, we show the calculated charge ratio of sea-level muons as a function of energy along with the recent experimental results.[4,40,42-46]

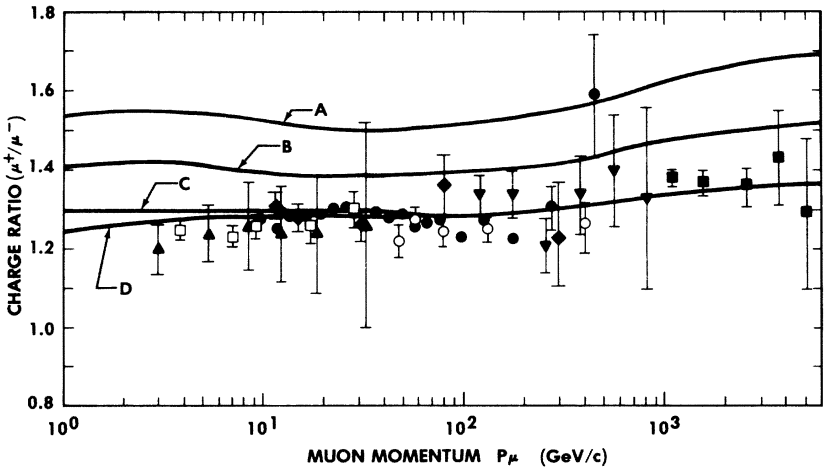

FIG. 6. The charge ratio of sea-level muons is shown as a function of muon momentum. The curves A and B in this figure show the calculated charge ratios from cosmic-ray proton-atmospheric collisions by (i) neglecting and (ii) by incorporating the charge-mixing parameter in nucleon-nucleus interactions respectively, and curve C after taking also into account the composition of primary cosmic rays. The data points in this figure are taken from the following: ● Ayre *et al.* (Ref. 4), ▼ Baxendale *et al.* (Ref. 40), ▲ Abdel-Monem *et al.* (Ref. 42), ◆ Allkofar *et al.* (Ref. 43), ○ Burnett *et al.* (Ref. 44), ■ Ashley *et al.* (Ref. 45), and □ Appleton *et al.* (Ref. 46).

Curve A in this figure is the ratio for the incident cosmic-ray protons calculated by using $w = 0.26$ for the charge transfer (exchange) probability. The shape of this curve can be understood as follows: The π^+/π^- production in pp collisions decreases from a value of 2.5 at 1 GeV/c to an asymptotic value of 1.66 above 50 GeV/c. Similarly the K^+/K^- ratio at production decreases from 6.4 at 1 GeV/c to 3.0 at 10 GeV/c and slowly reduces to an asymptotic value of 2.7 above 100 GeV/c. Therefore the slow decrease in the μ^+/μ^- ratio (curve A) from about 1.55 around 3 GeV/c to a minimum value ~40 GeV/c is a result of the decrease in the π^+/π^- ratio at production. The increase in the μ^+/μ^- ratio above 40 GeV/c is mostly due to the contribution of kaons and in part due to the increase in the muon production height in the atmosphere. Below about 5 GeV/c the contribution to sea-level muons also comes from pions produced at large atmospheric depths, where the charge-to-natural ratio of interacting nucleons decreases as a result of the charge transfer probability. This effect of w is responsible for the decrease in the charge ratio of muons below about 3 GeV/c in curve A. Curve B in Fig. 6 shows the effect of introducing the charge-mixing parameter for the nucleon-nuclei interactions (Sec. II). The effect of the energy dependence of this parameter is small on the charge ratio of muons above 1 GeV/c. The charge ratio of muons from interactions of deuterons and heavier nuclei is approximately unity, and is independent of energy. Curve C in Fig. 6 gives the charge ratio of muons after the inclusion of the charge composition of cosmic rays. The calculated charge ratio increases slowly from 1.28 at 1 GeV/c to 1.36 at 5000 GeV/c. One can notice that the calculated charge ratio (curve C) is in good agreement with the observed values above 10 GeV/c. However, below this momentum the observed data points are consistently lower. This discrepancy at low energies can be reduced (curve D) by requiring an energy-dependent charge-transfer probability as described in Sec. II.

The parameters which influence the charge of muons at sea level are (i) the charge ratios of pions and kaons at production, (ii) the charge-mixing parameter, η, in nucleon-nucleus collisions, (iii) the composition of incident cosmic rays, (iv) the charge-transfer probability, w, of the interacting nucleon, and to a lesser extent the interaction and attenuation mean free paths. The uncertainties in the production cross sections introduce an error of about 2% in the muon charge ratio at 1 GeV/c, while at 1000 GeV/c it is $\approx$3.3%. The uncertainties in the relative abundance of heavy nuclei including deuterons is about 10%. This error along with those in the interaction mean free paths lead to errors of 1% and 3.5% on μ^+/μ^- respectively at 1 and 1000 GeV/c. An error of 10% in the value of w propagates to 2.2% and 1.2% errors at 1 and 1000 GeV/c, respectively. One observes that the combined values of all these errors are well within the spread in the data points in Fig. 6. Therefore, we consider our calculated charge ratio (curve D) to be a good fit to the observed data.

VI. DISCUSSION

As already discussed in detail, the sea level muon momentum spectrum and charge ratio reflect the chemical composition of the primary cosmic rays and the characteristics of hadronic interactions. Thus, a comparison of our calculations with the observed experimental data will shed light on these characteristics.

We have already pointed out that our calculations of the sea level muon spectrum, without introducing any normalization, is in excellent agreement with the observed spectrum (Fig. 5) throughout the momentum range of 1–1000 GeV/c. Muons of energy greater than 150 GeV come from cosmic-ray nuclei of energy above ~1500 GeV, which is the limit for which direct experimental data on hadronic interactions is available. We thus feel that the observed cosmic-ray spectrum and charge composition can be extended along with the present representation of hadronic interaction characteristics to at least 10 TeV without any serious distortions.

The credibility of this conclusion can be further enhanced if one looks at the muon charge ratio as a function of momentum, because this ratio is a more sensitive parameter for exploring features of the chemical composition and of the hadronic interactions than is the absolute muon spectrum.[1-8] The data of Ayre *et al.*[4,39] between about 80 and 450 GeV/c in Fig. 6 show a significant decrease and a subsequent rise. Thompson[47] analyzed all of the vertical data between 2 and 1000 GeV/c and concluded that the charge ratio is constant in this interval. Burnett *et al.*,[44] by analyzing the data over a range of zenith angles, find the charge ratio to be constant above 25 GeV/c; Kasha *et al.*,[49] similarly find the charge ratio to be constant in the interval of 50 GeV/c to 2 TeV/c. We have thus chosen to disregard, in our discussion, the anomaly in the charge ratio reported by Ayre *et al.*[39] Combining all the data, including those of Ashley *et al.*,[45] between 1 and 8 TeV/c, we conclude that the muon charge ratio rises very slowly from 1 GeV/c to 8 TeV/c. (See Ref. 48 also.)

A comparison of our calculations with the above experimental data shows excellent agreement

TABLE II. A comparison of the theoretical predictions of the muon charge ratio.

	This calculation	Erlykin *et al.* Ref. 6	Liland Ref. 7	Morrison and Elbert Ref. 5	Adair Ref. 3	Hoffman Ref. 8
Spectral index of the proton	2.55 $E \leq 68$ GeV	2.62	2.75	2.70	2.70	2.75
	2.75 $E \geq 68$ GeV					
Energy spectrum $n/(p+n)$ in primary	0.105	0.136	...	0.095	0.11	0.11
π^+/π^- in pp collision	1.66	1.54	1.46	1.54	1.80	1.64[a]
π^+/π^- in p-air	1.38	1.54	1.27	1.46	...	1.646[b]
Energy dependence of σ_{in} in p-p	yes	no	no	yes	no	yes
μ^+/μ^- at 200 GeV/c	1.29	1.37	1.11	1.26	1.53	1.44
Error	0.03–0.05	0.07	...	0.07–0.11	0.11	0.16

[a] Using y^{proj} as the variable. He obtains 1.69 with $x_{\parallel}^*$ as the variable.
[b] Using a cascade model the ratio is 1.51.

throughout the momentum interval of 1 GeV/c to 5 TeV/c.[50] Thus, we find that if we make use of the experimentally determined production cross sections for pions and kaons in both the hadron-hadron and hadron-nucleus collision, and the observed cosmic-ray chemical composition, the absolute muon momentum spectrum as well as the muon charge ratio can be well understood in the momentum range 1 to 5000 GeV/c.[51]

Table II presents a comparison of our calculations with some of the previously calculated parameters relating to the muon charge ratio at 200 GeV/c. It may be mentioned that Frazer *et al.*,[1] Garraffo *et al.*,[2] and Yukutieli and Rotter[52] did not take into account the kaons and thus obtained values for the charge ratio which are ~10% lower than they should have been. Moreover, these calculations did not include the energy dependence of the inelastic pp cross section. Also, nuclear effects have been neglected by Frazer *et al.*[1] and by Yekutiele and Rotter.[52] These calculations are, therefore, not included in Table II.

The divergence of both the input data and the calculated charge ratio is apparent from this table. The ratio $n/(p+n)$ used in these calculations is nearly the same except for Erlykin *et al.*,[6] who made use of the low-energy relative abundances. Our calculated value of π^+/π^- in pp collisions is in good agreement with that of Hoffman,[8] but is higher than the values used by Liland,[7] Erlykin *et al.*,[6] and Morrison and Elbert[5]; the later authors did not use any Fermilab or ISR data. However, Adair[3] obtains a higher value of 1.8 for this ratio. The difference arises, we believe, because he has used only the cross section at fixed value of $p_\perp = 0.4$ GeV/c. It is thus somewhat difficult to understand why Hoffman's calculation differs from ours except that he used the coherent model to describe the nuclear target effects. Gibbs *et al.*[53] have shown that incoherent models such as that used by Adair[3] predict too many particles at very high energies, and yield a dependence of charge multiplicity on target atomic mass that is too flat. We believe that a similar situation may exist for the coherent-production model used by Hoffman.[8] It is clear that the value of π^+/π^- in p-air collisions obtained by Hoffman[8] in the framework of this model is too high when compared to the 200- and 300-GeV p-beryllium data.[20] Moreover, had Hoffman[8] used his cascade model, the calculated value would have been ~1.51 and he would have obtained a correspondingly lower value for the muon charge ratio.

We thus believe that the excellent agreement of our calculations with the experimental data in both the muon momentum spectrum and the charge ratio shows that there is no need at present to invoke any change in the cosmic-ray chemical composition or the nature of the hadronic interactions.

ACKNOWLEDGMENT

We would like to acknowledge the considerable help we have received from T. Ferbel. One of us (G.D.B.) has benefited from discussions with him on the invariant cross sections. We would also like to thank T. Cleghorn for useful comments.

APPENDIX

The production spectra of pions and kaons have been calculated as functions of atmospheric depth using Eq. (3) by taking into account the following aspects.

(i) Since the energy spectra of primary cosmic-ray nuclei are not simple power laws in kinetic energy per nucleon, they get modified during the

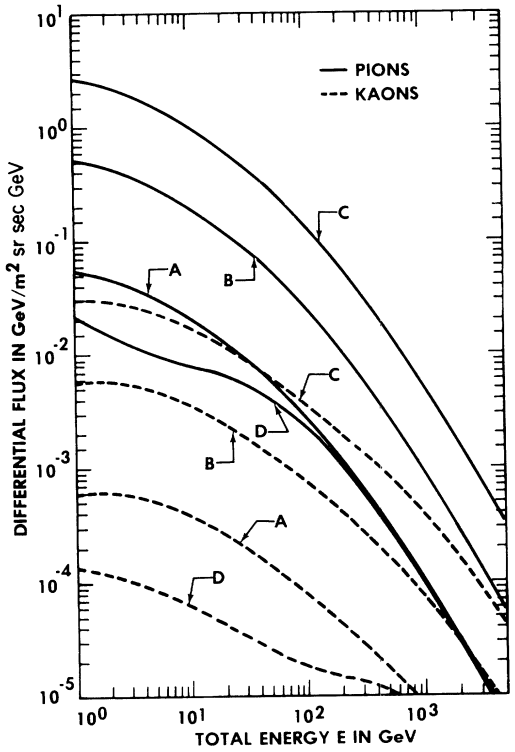

FIG. 7. The differential energy spectra of pions (solid curves) and kaons (dotted curves) in the atmosphere are shown, in energy flux units, at depths of 1 g cm^{-2} (curve A), 10 g cm^{-2} (curve B), 100 g cm^{-2} (curve C), and 1000 g cm^{-2} (curve D.

propagation in the atmosphere as a result of finite inelasticity. For this purpose we assumed an inelasticity of 0.5 and reduced the kinetic energy of the nucleons by a factor of 2 after each collision.

(ii) The charge composition of primary nuclei changes with atmospheric depth due to spallation. It is found from a simple calculation that the contribution of nuclei of charge ≥ 2 will be approximated to an equivalent number of helium nuclei without affecting the final results. In our calculations, we have assumed that on the average about 2.3 nucleons of the helium nuclei participate in the interaction[30] and the remaining nucleons leave without any change in their energy.

(iii) The π^+, π^- production spectra were taken to be identical to $[P_{\pi^+}(E,X)+P_{\pi^-}(E,X)]/2.0$ for nuclei of charge ≥ 2 and for deuterons. In the case of cosmic-ray protons, it was evaluated by first determining the fraction of interacting neutrons at a given atmospheric depth, using 0.5 as the charge transfer probability (Sec. III), and then by taking into account the effect of nucleon-nuclei interactions as described in Sec. II.

Using the production spectra thus derived as a function of atmospheric depth the equilibrium pion spectra in the atmosphere have been calculated. A similar procedure was also adopted for kaons except that the secondary production of kaons from interactions of pions and kaons was not incorporated; the contributions of this secondary production to the sea-level muon spectrum are negligible.

In Fig. 7, we show the spectra of pions $(\pi^+ + \pi^-)$ and kaons $(K^+ + K^-)$ for various atmospheric depths. One can notice from this figure that the pion spectra shown by the solid curves A, B, and C, at depths, 1, 10, and 100 g cm^{-2}, respectively, are

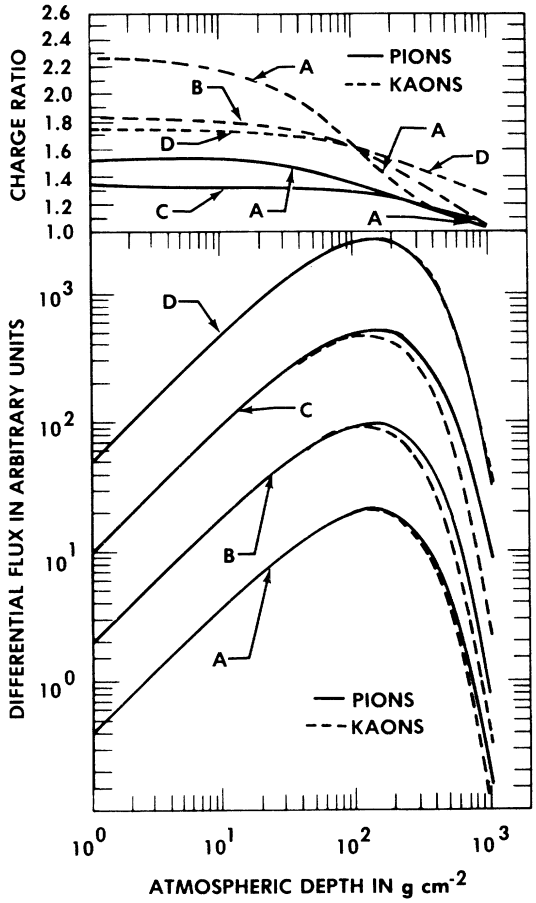

FIG. 8. The atmospheric growth curves for pions (solid curves) and kaons (dotted curves) in arbitrary flux units are shown in the lower part of this figure at fixed energies of 1 GeV (curve A), 10 GeV (curve B), 100 GeV (curve C), and 1000 GeV (curve D); the pion and kaon curves are normalized at 1 g cm^{-2} in order to bring out the differences. The upper part of this figure shows the variation of the charge ratio of pions (solid curves) and kaons (dotted curves) as a function of depth; labels on these curves are the same as those on the lower part of this figure.

nearly similar in their spectral shape over the entire energy range considered. However, the sea-level pion spectrum (curve *D*) deviates from the general spectral shape below about a hundred GeV as a result of the change in the atmospheric scale height which has been incorporated in our calculations. Similar behavior is seen in the case of kaons (dashed curves), except that the change in the spectral shape occurs at a higher energy, shifted by a factor of $(m_K\tau_\pi/m_\pi\tau_K)$ from that of pions. Here one may add that if the slow increase of the interaction mean free path of hadrons with energy were incorporated the flux of high-energy pions and kaons at large depths would be depleted.

We show, in Fig. 8, the atmospheric-depth dependence of the flux of pions (solid lines) and kaons (dashed curves), in arbitrary units, at energies 1, 10, 100, and 1000 GeV respectively by curves *A*, *B*, *C*, and *D*. By properly combining Fig. 7 and 8, one can easily obtain the flux of any one of the components at a given depth and energy. It can be seen from this Fig. 8 that the maximum flux value is reached between 100 g cm^{-2} and 200 g cm^{-2} of atmospheric depth. One can also notice that the higher the energy, the flatter the growth curve after the maximum is reached because the decay length becomes longer. It is evident that the growth curves for kaons (dashed curves) deviate from those of pions at large depths. For energies less than a few hundred GeV, the kaon growth curve is steeper because of the change in the atmospheric scale height (curve *D* of Fig. 7) and, to a lesser extent, of neglecting the production of kaons from pion interactions. On the contrary, at very high energies, say at 1000 GeV (curve *D*), the kaon growth curve is slightly flatter than that of pions because a large fraction of kaons even at sea level are those which were created at small atmospheric depths, and survived from interactions rather than from decay. As a result, the effect of neglecting the kaon production from pion interaction is more than compensated for by the longer interaction mean free path for kaons.

The charge ratios π^+/π^- and K^+/K^- are also shown as a function of depth in Fig. 8 by solid and dashed curves, respectively. Curves *A*, *B*, *C*, and *D* correspond respectively to energies 1, 10, 100, and 1000 GeV. One can notice that the pion charge ratio is nearly constant over one interaction mean free path for protons and slowly decreases as the depth increases. At energies $\lesssim 100$ GeV, the charge ratio reaches a value of $\simeq 1.05$ at sea level, while at higher energies this ratio slowly increases because at these energies a considerable fraction of the pions and kaons come from small atmospheric depths, where the charge ratio at production is high. This effect is very well seen in the case of kaons of 1000 GeV (dashed curve *D*). One can also notice the large value of K^+/K^- at 1 GeV at small atmospheric depths as a result of the low cross section for the production of K^- in *p*-*p* collisions at small energies.

---

*Work supported in part by NASA-NRC. On leave from Tata Institute of Fundamental Research, Bombay, India.

[1]W. R. Frazer, C. H. Poon, D. Silverman, and H. J. Yesian, Phys. Rev. D 5, 1653 (1972).
[2]Z. Garrafo, A. Pignotti, and G. Zgrablich, Nucl. Phys. B53, 419 (1973).
[3]R. K. Adair, Phys. Rev. Lett. 33, 115 (1974).
[4]A. Ayre *et al.*, in *Proceedings of the Thirteenth International Conference on Cosmic Rays, Denver, 1973* (Colorado Associated Univ. Press, Boulder, 1973), Vol. 3, p. 1822.
[5]J. L. Morrison and J. W. Elbert, in *Proceedings of the Thirteenth International Conference on Cosmic Rays, Denver, 1973* (Colorado Associated Univ. Press, Boulder, 1973), Vol. 3, p. 1833.
[6]A. D. Erlykin, L. K. Ng. and A. W. Wolfendale, J. Phys. A 7, 2059 (1974).
[7]A. Liland, in *Proceedings of the Fourteeth International Conference on Cosmic Rays, Munich, 1975* (Max Planck Institute for Extraterrestriche Physik, Munich, Germany, 1975), Vol. 6, p. 2088.
[8]H. J. Hoffman, Phys. Rev. D 12, 82 (1975).
[9]T. Ferbel, in Proceedings of the SLAC Summer Institute on Particle Physics, University of Rochester Report No. UR-500, 1974 (unpublished).
[10]H. Bøggild and T. Ferbel, Annu. Rev. Nucl. Sci. 24, 1 (1974).
[11]D. C. Carey *et al.*, Phys. Rev. Lett. 33, 327 (1974).
[12]J. Whitmore, Phys. Rep. 10C, 273 (1974).
[13]P. Capiluppi *et al.*, Nucl. Phys. B79, 189 (1974).
[14]E. Bracci, J. P. Droulez, E. Flaminco, J. D. Hansen, and D. R. O. Morrison, CERN Report No. CERN/HERA 73-1, 1973 (unpublished); N. Antinucci *et al.*, Lett. Nuovo Cimento 6, 121 (1973).
[15]E. Yen, Phys. Rev. D 10, 835 (1974).
[16]W. F. Baker *et al.*, Phys. Rev. Lett. 3, 101 (1961).
[17]D. Dekkers *et al.*, Phys. Rev. B137, 962 (1964).
[18]J. V. Allaby *et al.*, CERN Report No. CERN-EXP-70-12, 1970 (unpublished).
[19]T. Eichten *et al.*, Nucl. Phys. B44, 333 (1972).
[20]W. F. Baker *et al.*, Phys. Lett. 51B, 303 (1974).
[21]We would like to note that because of the steep cosmic-ray spectrum, it is the value of $E(d^3\sigma/d^3p)$ around $x_\parallel^* \approx 0.2$, which is important.
[22]R. D. Edge, D. H. Tompkins, and J. W. Gleen, Nuovo Cimento 31, 641 (1976).
[23]A. C. Melissinos *et al.*, 128, 2372 (1962).
[24]A. Ayre *et al.* (Ref. 4), using the data for Be and Al targets at two fixed values of $x_\parallel^*$, invoked that in 32% of the *pn* collisions, the charge ratio of pions is determined by *nn* collisions.

[25]L. Stutte, Bull. Am. Phys. Soc. 18, 665 (1973).
[26]M. J. Ryan, J. F. Ormes, and V. K. Balasubrahmanyan, Phys. Rev. Lett. 28, 985 (1972).
[27]W. R. Webber and J. A. Lezniak, Astrophys. Space Sci. 30, 361 (1975).
[28]E. Juliusson, Astrophys. J. 191, 331 (1974).
[29]S. N. Ganguli and B. V. Sreekantan, *Proceedings of the Fourteenth International Conference on Cosmic Rays, Munich, 1975* (Max Planck Institut für Extraterrestriche Physik, Munich, Germany, 1975), Vol. 2, p. 570.
[30]M. V. K. Appa Rao, R. F. Daniel, and K. A. Neelakantan, Proc. Ind. Acad. Sci. 43A, 181 (1956).
[31]Y. Pal and B. Peters, K. Dan. Vidensk. Selek. Mat.-Fys. Medd. 33, 1 (1964).
[32]R. R. Daniel, N. Durgaprasad, P. K. Malhotra, and B. Vijayalakshmi, Nuovo Cimento Suppl. 1, 1169 (1963).
[33]F. T. Dao *et al.*, Phys. Rev. D 10, 3588 (1974).
[34]G. Bellettini, *et al.*, Nucl. Phys. 79, 609 (1966).
[35]W. R. Webber, Nuovo Cimento 4, 1285 (1956).
[36]N. B. Schmidt *et al.*, Phys. Lett. 50B, 1 (1974).
[37]R. R. Daniel and S. A. Stephens, Rev. Geophys. Space Phys. 12, 233 (1974).
[38]O. C. Allkofer, K. Carstensen, and W. D. Dau, in *Proceedings of the Twelfth International Conference on Cosmic Rays, Hobart, 1971,* edited by A. G. Fenton and K. B. Fenton (Univ. of Tasmania Press, Hobart, Tasmania, 1971), Vol. 4, p. 1314.
[39]C. A. Ayre *et al.*, in *Proceedings of the Thirteenth International Conference Cosmic Rays, Denver, 1973* (Colorado Associated Univ. Press, Boulder, 1973), Vol. 3, p. 1754.
[40]T. M. Baxendale *et al.*, in *Proceedings of the Fourteenth International Conference on Cosmic Rays, Munich, 1975* (Max Planck Institut für Extraterrestriche Physik, Munich, Germany, 1975), Vo. 6, p. 2011.
[41]B. C. Nandi and M. S. Sinha, J. Phys. A 5, 1384 (1972).
[42]M. S. Abdel-Monen, J. R. Benbrook, A. R. Osborne, W. R. Sheldon, N. M. Duller, and P. J. Green, in *Proceedings of the Thirteenth International Conference on Cosmic Rays, Denver, 1975* (Colorado Associated Univ. Press, Boulder, 1973), Vol. 3, p. 1811.
[43]O. C. Allkofer, K. Carstensen, W. D. Dau, E. Fahnders, W. Heinrich, and H. Jokioch, in *Proceedings of the Twelfth International Conference on Cosmic Rays, Hobart, 1971,* edited by A. G. Fenton and K. B. Fenton (Univ. of Tasmania Press, Hobart, Tasmania, 1971), Vol. 4, p. 1319.
[44]T. H. Burnett, L. J. LaMay, G. E. Masek, T. Maung, E. S. Miller, H. Ruderman, and W. Vernon, Phys. Rev. Lett. 30, 937 (1973).
[45]G. K. Ashley II, J. W. Keuffel, and M. O. Larson, Phys. Rev. D 12, 20 (1975).
[46]I. C. Appleton, M. T. Hoque, and B. C. Rastin, Nucl. Phys. B26, 365 (1971).
[47]M. G. Thompson, in *Cosmic Rays at Ground Level*, edited by A. W. Wolfendale (International Scholarly Book Service, Portland, 1974), pp.44–48.
[48]B. C. Nandi and M. S. Sinha, Nucl. Phys. B40, 289 (1972).
[49]H. Kasha, R. Kellogg, B. Higgs, L. Leipuner, and R. Larson, in *Proceedings of the Fourteenth International Conference on Cosmic Rays, Munich, 1975* (Max Planck Institut für Extraterrestriche Physik, Munich, Germany, 1975), Vol. 6, p. 1868.
[50]It is interesting to point out that the direct production of muons in high-energy interactions could influence the charge ratio at large momentum values. However, making use of the 400-GeV data by L. B. Leipuner *et al.*, Phys. Rev. Lett. 35, 1613 (1975), and assuming that its production spectrum is similar to that of pions, we found that the contribution of prompt muons to the total muon spectrum at sea level is $<10^{-4}$ below 100 GeV/c and increases to a value of about 1% at 5000 GeV/c.
[51]A similar conclusion was drawn from the preliminary results of these calculations reported elsewhere: G. D. Badhwar, S. A. Stephens, and R. L. Golden, in *Proceedings of the Fourteenth International Conference on Cosmic Rays, Munich, 1975* (Max Planck Institut für Estraterrestrische Physik, Munich, Germany, 1975), Vol. 6, p. 2077.
[52]G. Yekutieli and Sh. Rotter, Phys. Lett. 47B, 36 (1973).
[53]R. E. Gibbs, J. R. Florian, L. D. Kirkpatrick, J. J. Lord, and J. W. Martin, Phys. Rev. D 10, 783 (1974).